Electronic Supplementary Material (ESI) for Soft Matter.

Supplementary Information for

Engineering interfacial entropic effects to generate giant viscosity changes in nanoparticle embedded polymer thin films

Aparna Swain[1], Nafisa Begam[1], Sivasurender Chandran[2], M. S. Bobji[3], and J. K. Basu[1*]

[1] Department of Physics, Indian Institute of Science, Bangalore, 560 012, India,
[2] Institute of Physics, University of Freiburg, 79104 Freiburg, Germany
[3] Department of Mechanical Engineering, Indian Institute of Science, Bangalore, 560012, India,

1. Characterization of PGNPs

In this report, we have performed viscosity measurements on polymer nanocomposite thin films using force-distance spectroscopy. The composites consist of thiol terminated polystyrene (PS-SH) grafted gold nanoparticles (PGNP) dispersed in polystyrene [1]. PGNPs were synthesized using *in-situ* grafting-to method [2]. Two different grafted chain lengths and one matrix chain length were taken for the measurements. We obtained the size of the PGNP core from transmission electron microscopy (TEM) (see Fig. S1). The mean diameter of the gold core, obtained from the statistical analysis of the TEM images, are 2.2 ±0.3 nm and 1.1 ± 0.3 nm for the PGNPs grafted with PS-SH of molecular weight 3kDa and 20kDa, respectively.

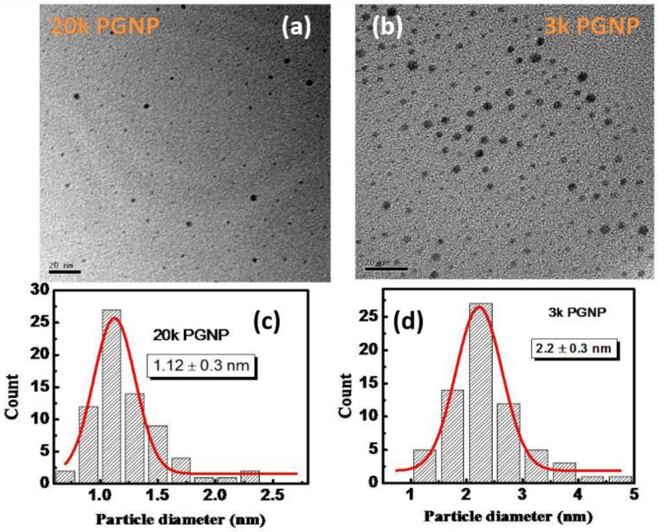

Fig. S1: TEM images of PGNPs grafted with (a) *20kDa PS-SH and* (b) *3kDa PS-SH. Respective histograms of the core size distribution are shown for PGNPs grafted with* (c) *20kDa and* (d) *3kDa PS-SH.*

Small a he
total dr of

PGNPs. The overall PGNP diameters (= $2\pi/q_{max}$, where q_{max} is the peak position highlighted with the arrows in Fig. S2) as obtained were noted in the respective panels.

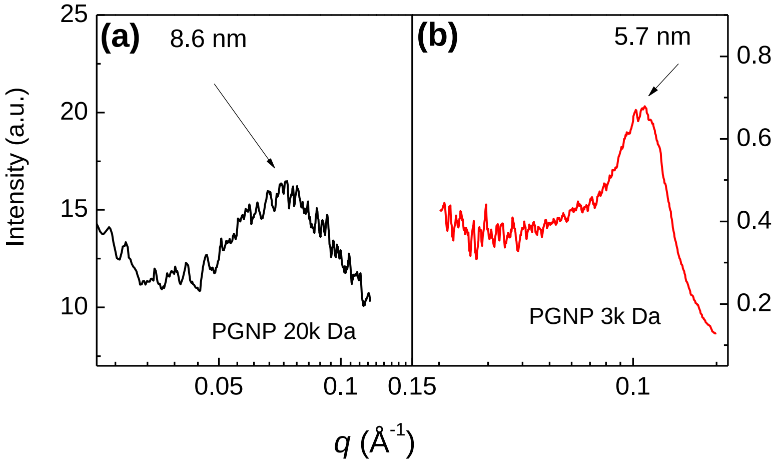

Fig. S2: SAXS intensity profiles showing the PGNP diameters for the grafted chain of molecular weight 20kDa (a) and 3kDa (b).

2. Dispersion state of PGNPs in PS matrix:

We performed scanning electron microscopy (SEM) on all the PNC films at room temperature to investigate the dispersion state of the PGNPs in the PS matrix. The SEM images indicate that the films, especially the surface of the films (~10 nm, penetration depth of the electrons) are well dispersed even at such high volume fractions of the PGNPs. Inter-particle distances for all the samples were measured from the SEM images obtained at room temperature. Typical SEM images and their inter-particle distances are shown in the Fig. S3.

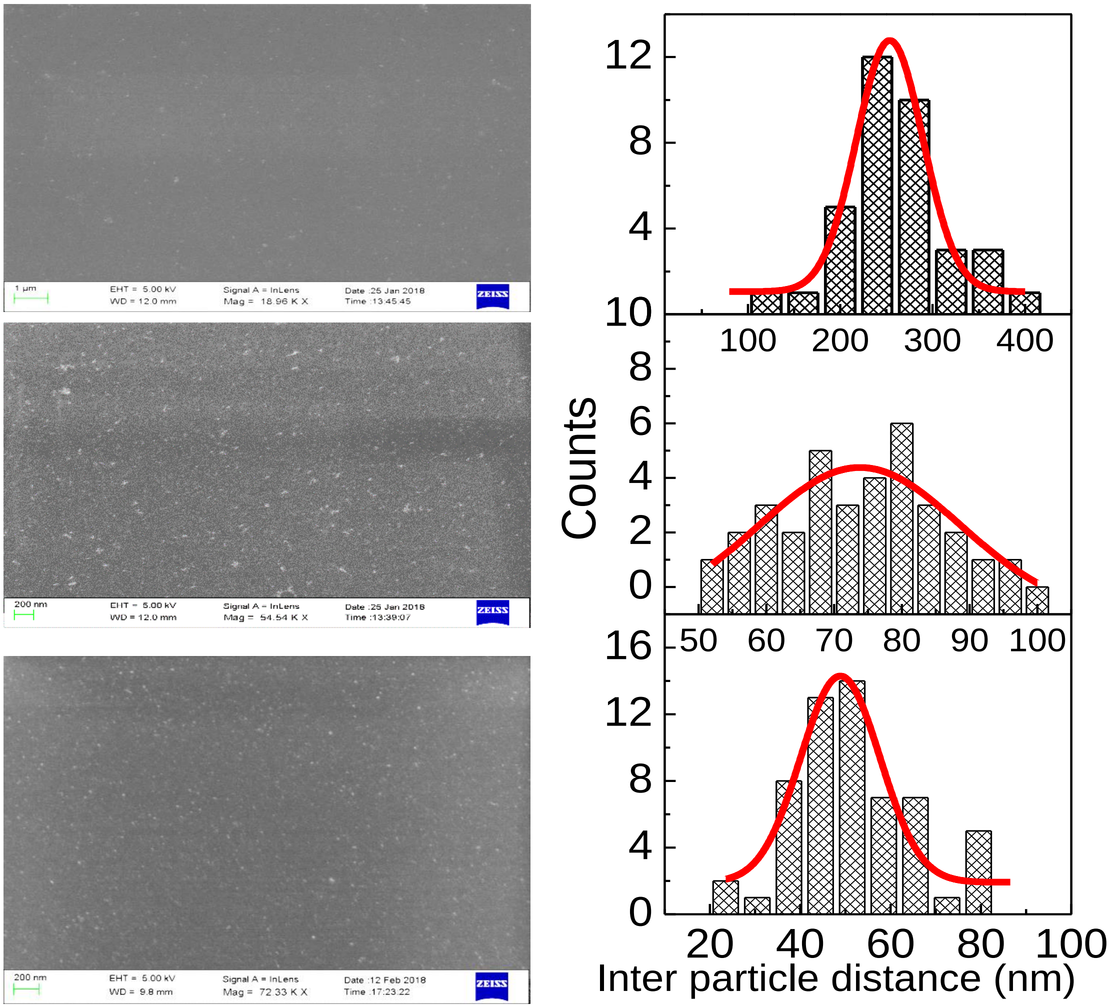

Fig. S3: SEM images for the sample (top) PNC$_{0.15}$ (0.20), (middle) PNC$_{0.15}$ (0.34) and (bottom) PNC$_{1}$ (0.90) representing the typical dispersion state of all the samples in table 1 of the main manuscript. Respective histograms of the inter-particle distances (*h*) are shown on the right panels.

3. Calculation of volume fractions PGNPs in PNCs:

First we obtained the mass fractions of the gold core in PGNPs using TGA data as shown in Fig. S4. In these data, the mass of the nanoparticles after heating to a very high temperature, which is the mass of the leftover gold cores, divided by the initial mass of the sample provides the fraction of the gold core in a PGNP. As determined from TGA, the gold mass fractions are 0.45 and 0.08 for PGNPs with grafted chains 3kDa and 20kDa, respectively. Using these values along with the core and total diameters obtained from TEM and SAXS data, we estimated the total PGNP volume fractions in a PNC. For example, let us say M_{NP} (mg) of PGNP with 3kDa was mixed with M_{PS} (mg) of PS chains in a certain amount of solvent. The total concentration (PGNP+PS) of the solution determines the thickness of the film obtained using spin-coating method.

Therefore, the mass of the only cores = $M_{core} = M_{NP}*0.45$ (mg)

- ⇨ Volume of the core, $V_{core} = M_{core}/\rho_{Au}$ (in cc)
  Where, ρ_{Au} is the mass density of the Au = 19.3 g/cc
  Similarly, volume of the corona, $V_{corona} = M_{NP}* (1-0.45) / \rho_{PS}$ (in cc)
  Where, ρ_{PS} is the mass density of bulk PS = 1.04 g/cc.
  Volume of the matrix chains, $V_{matrix} = M_{PS}/ \rho_{PS}$
- ⇨ The volume fraction of the total PGNP $\boldsymbol{\phi = (V_{core} + V_{corona}) / (V_{core} + V_{corona} + V_{matrix})}$

The table 1 in the main manuscript shows the value of ϕ for each PNCs obtained using the above mentioned method.

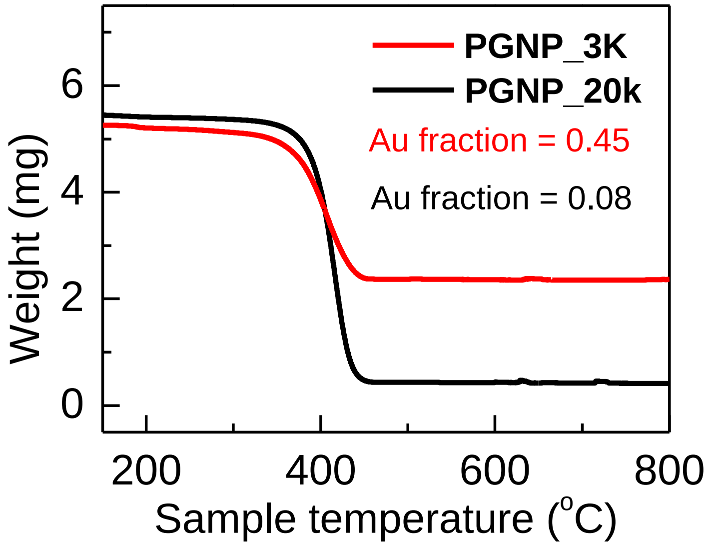

Fig. S4: TGA data showing the mass fraction of the gold core in the PGNPs for both the grafted chains.

4. Comparison of F-D Curves collected on Si and PS 20k:

As a preliminary test, we collected temperature dependent F-D curves on a silicone substrate and compared with that of a pure PS film. Temperature dependent F-D curves for silicon substrate are shown in Fig. S5(a) whereas, the same for PS20k films are shown in Fig. S5 (b). We can see that the F-D curves on silicon show a sudden drop of the pull-off force indicating no liquid bridge and hence no viscous behavior as is expected in the case of such a hard substrate. Along the expected line, the data does not have any temperature influence. On the contrary, the F-D curves on the PS20k and PNCs films (see Fig. S5 (b) and Fig. 2 in the main manuscript) exhibit the well-shaped liquid bridge on the F-D curves indicating a liquid (viscous/capillary) like property.

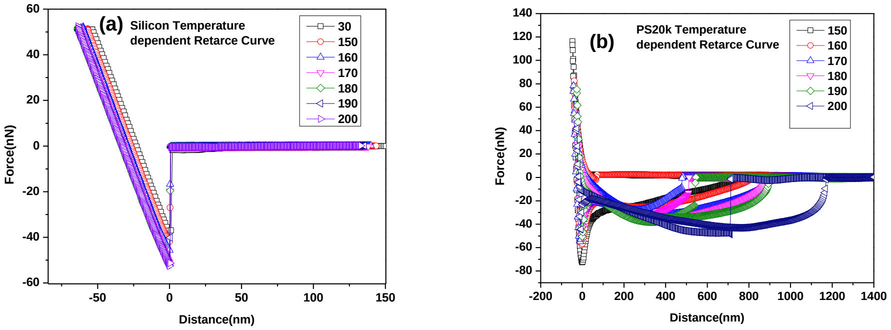

Fig. S5: F-D Curves as a function of temperature (a) on silicon substrate showing the property of a hard surface, and (b) on a PS20kDa film exhibiting clear liquid bridge as expected for liquid-like films.

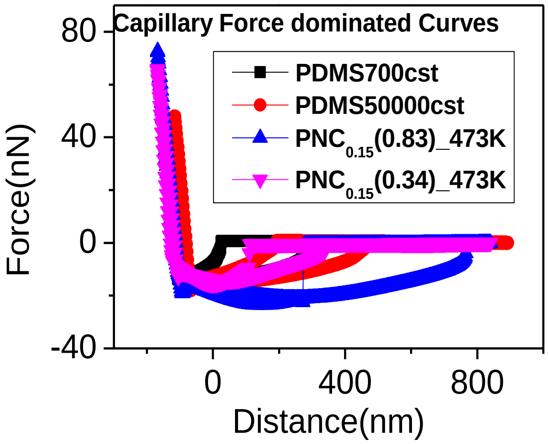

Fig. S6: Comparison of the F-D curves of PS and PNC (with *f* = 0.15) films with that of PDMS films showing similar shape and magnitude of pull-off force indicating a capillary force dominated regime of the force.

5. Viscosity extraction for the reference sample PDMS

As a reference, we have carried out the F-D curve measurements on thick polydimethylsiloxane (PDMS) films (spin coated onto a silicon substrate) of known viscosities of 50 and 0.7 Ns/m^2. For consistency, we maintained the tip velocity (200 nm/s) as that of our experiments on PS films. As shown in Fig. S7, we have modeled (red solid lines) the appropriate region of the data (black squares) using equation 4 of the main manuscript. For modeling, we used the surface tension of PDMS and the contact angle of PDMS on a silicon surface obtained from the literature [3,4]. All other parameters were varied to get a better fit to the data. The parameters as obtained from our fitting are summarized in the table below. Clearly, our analysis resulted in the corresponding viscosities as 44 ± 17 Ns/m^2, and 1.3 ± 0.6 Ns/m^2 which are close to the expected values (50 and 0.7 Ns/m^2).

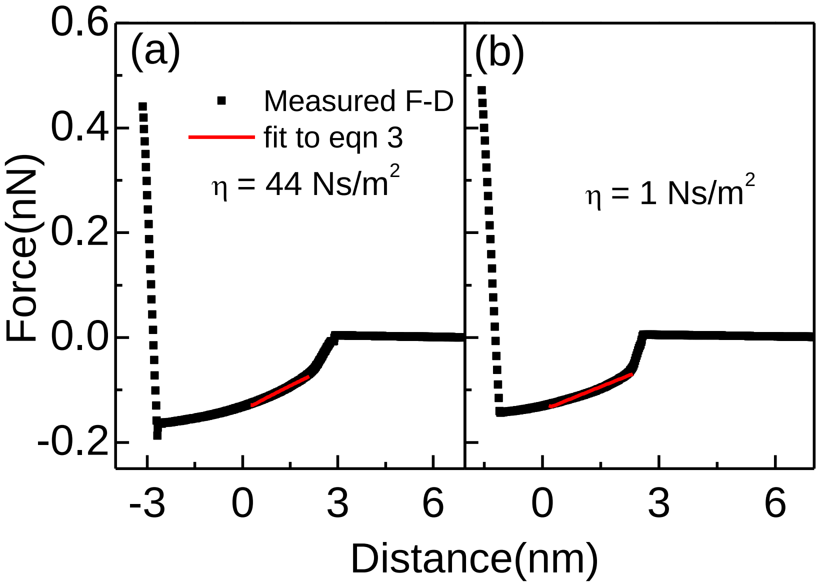

Fig. S7: F-D curves collected (symbols) on thick PDMS films with known viscosity (a) 50, and (b) 0.7 Ns/m^2, respectively, and the corresponding model fit (red solid line) of equation 4 of the main manuscript.

Films	A	x0	b0	Contact angle	Surface tension	Viscosity	Liquid bridge radius	Volume of the liquid bridge	Velocity of the tip
PDMS 50	-1.5* 10^{-8} N	0.31nm	-0.1 nm	101°	0.0157 N/m	44 Ns/m^2	180 nm	4500 nm^3	200 nm/s
PDMS 0.7	-4.7* 10^{-8} N	0.23 nm	-0.1 nm	101°	0.0157 N/m	1.3 Ns/m^2	130	5300 nm^3	200 nm/s

6. Extraction of the liquid-bridge radius

Extracted values of *R* obtained from the modelling of the PS F-D curves are shown in Fig. S8.

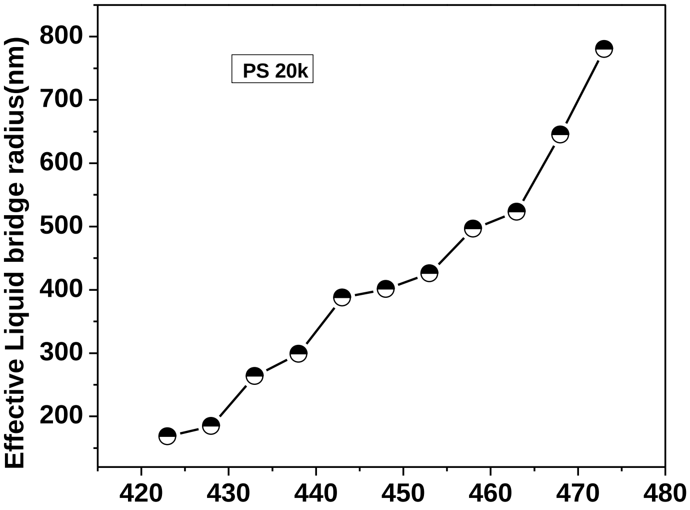

Fig. S8: Effective radius of liquid bridge, *R* vs temperature for pristine PS film shows a monotonic increase with temperature.

We used these *R* values at different temperatures (obtained from PS) in the analysis of PNC data as the initial values of the fit parameter *R* and then fitted the PNC F-D curves iteratively such that there is no change in the values of viscosity with *R*. We plotted the extracted *R* for the PNC films in Fig. S9.

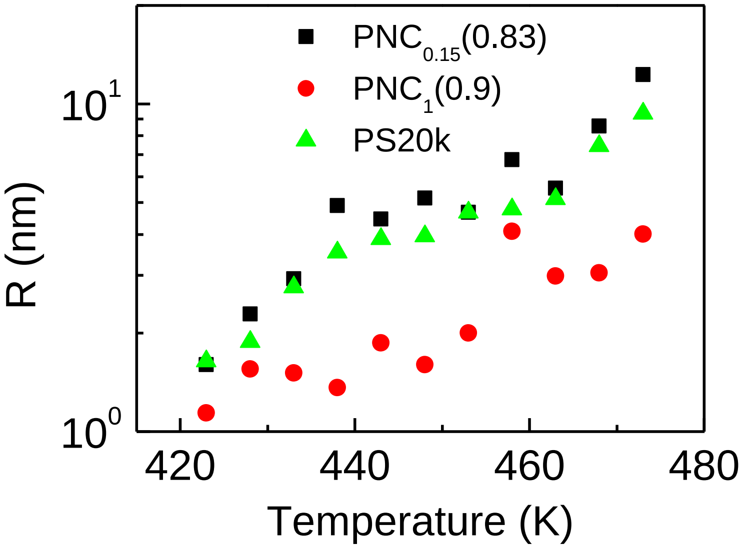

Fig. S9: Typical liquid bridge radius *R* obtained from the fit for two PNCs as indicated by the legends.

The volume of liquid bridge, *V*, for PNCs with high ϕ are compared with the pure PS values in Fig. S10. We can see in Fig. S10 that the volume of liquid bridge, V increases with increasing temperature, i.e. with decreasing viscosity.

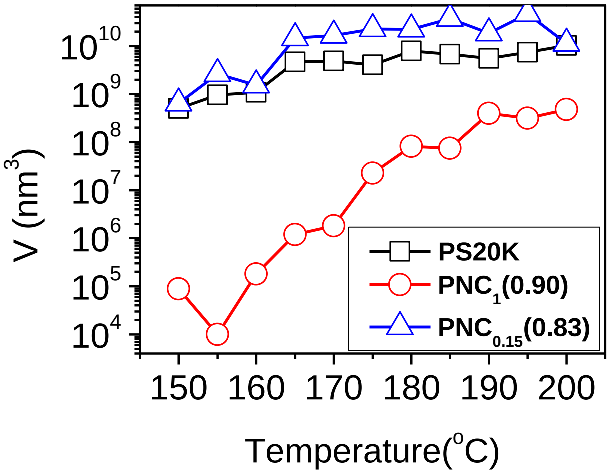

Fig. S10: Volume of the liquid bridge, V as a function of temperature showing an increase with decreasing viscosity.

7. Details of all the parameters obtained from F-D curve fitting:

On modelling the data, we have used the temperature dependent *R* values, extracted from the PS F-D curve fits, as the initial value of the fit parameter, *R*, for the PNCs. We have fitted the data iteratively until the viscosity value stabilizes. Tables showing all the parameter values are provided below. Here, the parameters in i*talic font* represent the fixed ones and **bold font** parameters are the ones obtained from the fit.

Table for PS20k

Temp(K)	**A (N)**	**b0 (m)**	**x0 (m)**	*η(Ns/m^2)*	*γ(N/m)*	**Volume (m^3)**	**R (m)**
423	**$-1.86*10^{-8}$**	**$-1*10^{-8}$**	**$-1.8*10^{-8}$**	*1063.7*	*0.0309*	**$4.9*10^{-19}$**	**$1.64*10^{-7}$**
428	**$-3.20*10^{-8}$**	**$-1*10^{-8}$**	**$-1.3*10^{-8}$**	*639.7*	*0.0306*	**$6*10^{-19}$**	**$1.88*10^{-7}$**
433	**$-3.20*10^{-8}$**	**$-1*10^{-8}$**	**$-1.1*10^{-8}$**	*343*	*0.0302*	**$1*10^{-18}$**	**$2.76*10^{-7}$**
438	**$-1.05*10^{-7}$**	**$-1.1*10^{-8}$**	**$-5.2*10^{-8}$**	*194.6*	*0.0298*	**$4.6*10^{-18}$**	**$3.53*10^{-7}$**
443	**$-7.63*10^{-8}$**	**$-1*10^{-7}$**	**$3*10^{-8}$**	*116.9*	*0.0294*	**$4.9*10^{-18}$**	**$3.87*10^{-7}$**
448	**-8.00E-08**	**$-1*10^{-8}$**	**3.8E-08**	*72.5*	*0.029*	**$7.9*10^{-18}$**	**$3.95*10^{-7}$**
453	**$-9.40*10^{-8}$**	**$-1*10^{-8}$**	**0.0**	*46*	*0.0287*	**$6.8*10^{-18}$**	**$4.67*10^{-7}$**
458	**$-8.20*10^{-8}$**	**$-1*10^{-8}$**	**0.0**	*31.6*	*0.0283*	**$5.9*10^{-18}$**	**$4.77*10^{-7}$**
463	**$-6.80*10^{-8}$**	**$-1*10^{-8}$**	**$-1*10^{-9}$**	*23.7*	*0.0279*	**$5.9*10^{-18}$**	**$5.13*10^{-7}$**
468	**$-5.30*10^{-8}$**	**$-1*10^{-8}$**	**$-1*10^{-9}$**	*15*	*0.0275*	**$7.4*10^{-18}$**	**$7.45*10^{-7}$**
473	**$-4.50*10^{-8}$**	**$-1*10^{-7}$**	**$-1*10^{-9}$**	*10*	*0.0272*	**$1*10^{-17}$**	**$9.35*10^{-7}$**

Table for PNC$_{0.15}$(0.83)

Temp(K)	**A (N)**	**b0 (m)**	**x0 (m)**	**η(Ns/m^2)**	*γ(N/m)*	**Volume (m^3)**	**R (m)**
423	**$-4.2*10^{-9}$**	**$-9.4*10^{-9}$**	**$2.5*10^{-8}$**	**461.1**	*0.0309*	**$6.4*10^{-20}$**	**$1.66*10^{-7}$**
428	**$-5.2*10^{-8}$**	**$-3.9*10^{-9}$**	**$1.3*10^{-8}$**	**95.2**	*0.0306*	**$2.6*10^{-18}$**	**$2.29*10^{-7}$**
433	**$-3.2*10^{-8}$**	**$-1*10^{-8}$**	**$3.8*10^{-8}$**	**86**	*0.0302*	**$1.6*10^{-18}$**	**$2.93*10^{-7}$**
438	**$-8.9*10^{-8}$**	**$-3.2*10^{-9}$**	**$2.7*10^{-8}$**	**28.6**	*0.0298*	**$1.5*10^{-17}$**	**$4.9*10^{-7}$**
443	**$-1*10^{-7}$**	**$-6.5*10^{-9}$**	**$2.8*10^{-8}$**	**12.6**	*0.0294*	**$1.7*10^{-17}$**	**$4.49*10^{-7}$**
448	**$-1.5*10^{-7}$**	**$-1*10^{-9}$**	**$3.5*10^{-8}$**	**4.6**	*0.029*	**$8.2*10^{-18}$**	**$5.17*10^{-7}$**
453	**$-1.2*10^{-7}$**	**$-1*10^{-9}$**	**$1.5*10^{-8}$**	**2.4**	*0.0287*	**$2.2*10^{-17}$**	**$4.67*10^{-7}$**
458	**$-1.1*10^{-7}$**	**$-1*10^{-9}$**	**$5.8*10^{-8}$**	**5.4**	*0.0283*	**$1.7*10^{-17}$**	**$6.75*10^{-7}$**
463	**$-8.6*10^{-8}$**	**$-1*10^{-8}$**	**$1*10^{-8}$**		*0.0279*	**$1.9*10^{-17}$**	**$5.54*10^{-7}$**
468	**$-1.3*10^{-7}$**	**$-1*10^{-9}$**	**$3.4*10^{-8}$**		*0.0275*	**$1.2*10^{-17}$**	**$8.56*10^{-7}$**
473	**$-3.9*10^{-8}$**	**$-1*10^{-8}$**	**$1.1*10^{-8}$**		*0.0272*	**$1.1*10^{-17}$**	**$1.23*10^{-6}$**

Table for PNC$_1$(0.9)

Temp(K)	**A (N)**	**b0 (m)**	**x0 (m)**	**η(Ns/m^2)**	*γ (N/m)*	**Volume (m^3)**	**R (m)**
423	**$-3.7*10^{-7}$**	**$2.1*10^{-8}$**	**$1.5*10^{-7}$**	**$1.6*10^{6}$**	*0.0309*	**$8.5*10^{-23}$**	**$1.14*10^{-7}$**
428	**$-1.8*10^{-7}$**	**$-8.9*10^{-8}$**	**$3.9*10^{-8}$**	**809725.6**	*0.0306*	**$2.5*10^{-22}$**	**$1.55*10^{-7}$**
433	**$-1.1*10^{-7}$**	**$-1*10^{-8}$**	**$1*10^{-7}$**	**283779.1**	*0.0302*	**$1.8*10^{-22}$**	**$1.5*10^{-7}$**
438	**$-4*10^{-8}$**	**$-1*10^{-7}$**	**$6.3*10^{-8}$**	**281631.7**	*0.0298*	**$1.2*10^{-21}$**	**$1.36*10^{-7}$**
443	**$-4.5*10^{-8}$**	**$-1*10^{-7}$**	**$9.4*10^{-8}$**	**153926.9**	*0.0294*	**$1.8*10^{-21}$**	**$1.87*10^{-7}$**
448	**$-8.9*10^{-9}$**	**$-1.3*10^{-7}$**	**$7.5*10^{-8}$**	**119041.9**	*0.029*	**$2.3*10^{-20}$**	**$1.6*10^{-7}$**
453	**$-2.2*10^{-8}$**	**$-1*10^{-7}$**	**$7.1*10^{-8}$**	**47164.6**	*0.0287*	**$8.6*10^{-20}$**	**$2.0*10^{-7}$**
458	**$-1.2*10^{-8}$**	**$-3*10^{-7}$**	**0.0**	**37393.1**	*0.0283*	**$1*10^{-24}$**	**$4.09*10^{-7}$**
463	**$-2.1*10^{-8}$**	**$-3*10^{-7}$**	**$5.3*10^{-9}$**	**21512.3**	*0.0279*	**$4.0*10^{-19}$**	**$2.98*10^{-7}$**
468	**$-5.1*10^{-8}$**	**$-1*10^{-7}$**	**$5.8*10^{-8}$**	**6547.5**	*0.0275*	**$3.2*10^{-18}$**	**$3.05*10^{-7}$**
473	**$-6.5*10^{-8}$**	**$-3.9*10^{-8}$**	**$3.1*10^{-8}$**	**576.6**	*0.0272*	**$4.8*10^{-18}$**	**$4.01*10^{-7}$**

8. Normalized viscosity vs T_g

Motivated by the orders of magnitude variations in viscosity for the changes in glass transition temperature, we have plotted the normalized viscosity as a function of normalized T_g in Fig. 6 of the main manuscript on a semilogarithmic scale. A nice collapse of the data is suggestive of an exponential dependence of the normalized viscosity with the normalized glass transition temperature.

We have also plotted the normalized viscosity on a log-log scale in Fig. S11 to visualize a possible power law dependence of viscosity on T_g. In this way we extract a very high exponent of *ca* 50, which again is a suggesting an exponential dependence of the normalized viscosity.

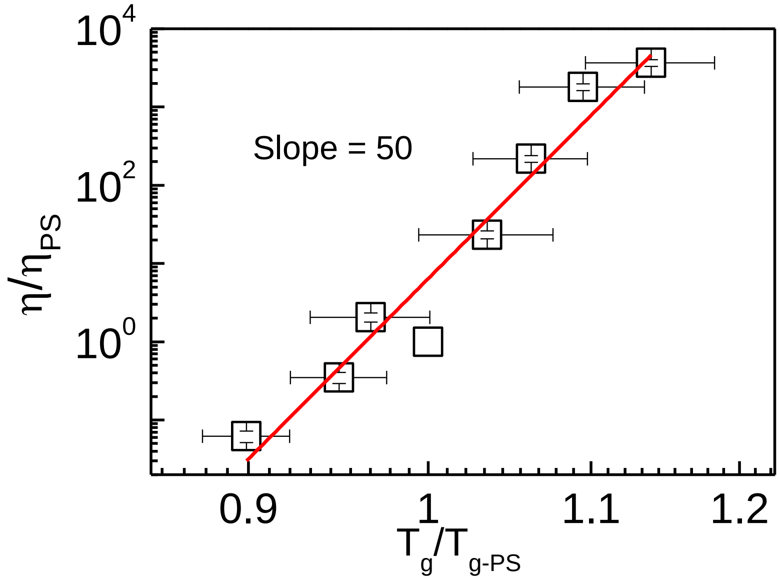

Fig. S11: Normalized viscosity for all the samples on a double logarithmic scale (right panel) scale showing an exponential dependence on normalized T_g.

9. Calculation of PNC viscosity from Wang and Hill model

We have compared our results with the theoretical prediction of Wang and Hill [5]. In this model, the intrinsic viscosity is given by [6]

$$[\eta] = \lim_{\varphi \to 0} \frac{\eta_{PNC} - \eta_{PS}}{\varphi\, \eta_{PS}} \quad \text{---} \quad (3)$$

Where, $[\eta]$ can be calculated using the relation

$$[\eta] = \frac{(A'\chi^2 + B'\chi + C') + ka(D'\chi^2 + E'\chi + F')}{(A\chi^2 + B\chi + C) + ka(D\chi^2 + E\chi + F)} \quad \text{---------------------------------} \quad (4)$$

$$\text{And, } A = -480a^{13} - 800a^{10}a'^3 + 900a^6a'^7 + 380a^3a'^{10}$$

$$B = 960a^{13} - 400a^{10}a'^3 + 300a^6a'^7 + 890a^3a'^{10}$$

$$C = -480a^{13} + 1200a^{10}a'^3 - 1200a^6a'^7 + 480a^3a'^{10}$$

$$D = 96a^{13} + 400a^{10}a'^3 - 672a^8a'^5 + 450a^6a'^7 + 76a^3a'^{10}$$

$$E = -192a^{13} + 200a^{10}a'^3 - 336a^8a'^5 + 150a^6a'^7 + 178a^3a'^{10}$$

$$A' = -1200a^{10}a'^3 - 2000a^7a'^6 + 2250a^3a'^{10} + 950a'^{13}$$

$$B' = 400a^{10}a'^3 + 4000a^7a'^6 - 2500a^3a'^{10} - 150a'^{13}$$

$$C' = 800a^{10}a'^3 - 2000a^7a'^6 + 2000a^3a'^{10} - 800a'^{13}$$

$$D' = 240a^{10}a'^3 + 1000a^7a'^6 - 1680a^5a'^8 + 1125a^3a'^{10} + 190a'^{13}$$

$$E' = -80a^{10}a'^3 - 200a^7a'^6 + 3360a^5a'^8 - 1250a^3a'^{10} - 30a'^{13}$$

$$F' = -160a^{10}a'^3 + 1000a^7a'^6 - 1680a^5a'^8 + 1000a^3a'^{10} - 160a'^{13}$$

$$a' = a + \delta$$

$$\frac{\delta}{R_g} = \alpha\beta\left(\frac{R_g}{d_t}\right)\{1 - \exp[-ah(\varphi)/(\beta R_g)]\} \text{ -------------------------------- (5)}$$

Here, $\alpha = 0.4$ *and* $\beta = 10, d_t = 9.4$ nm *and* $R_g = 10$ nm for PS20k

$$h(\varphi) = [\left(\frac{0.638}{\varphi}\right)^{1/3} - 1] \text{ --- (6)}$$

and $\chi = (\eta^i/\eta^0)/(\rho^i/\rho^0)$, --- (7)

Here η^0 and ρ^0 are the viscosity and density of the pure melt.

Using the above equation, we have calculated the intrinsic viscosity of PNCs with varying χ.

Some typical plots of $[\eta]$ as function of ϕ with varying χ are shown in Fig. S12(a).

In order to estimate the viscosity, we have used the value of η_0 equals to the viscosity of pure PS of molecular weight 19k [7] from the literature and used the relation 3. Estimated η is shown in Fig. S12(b).

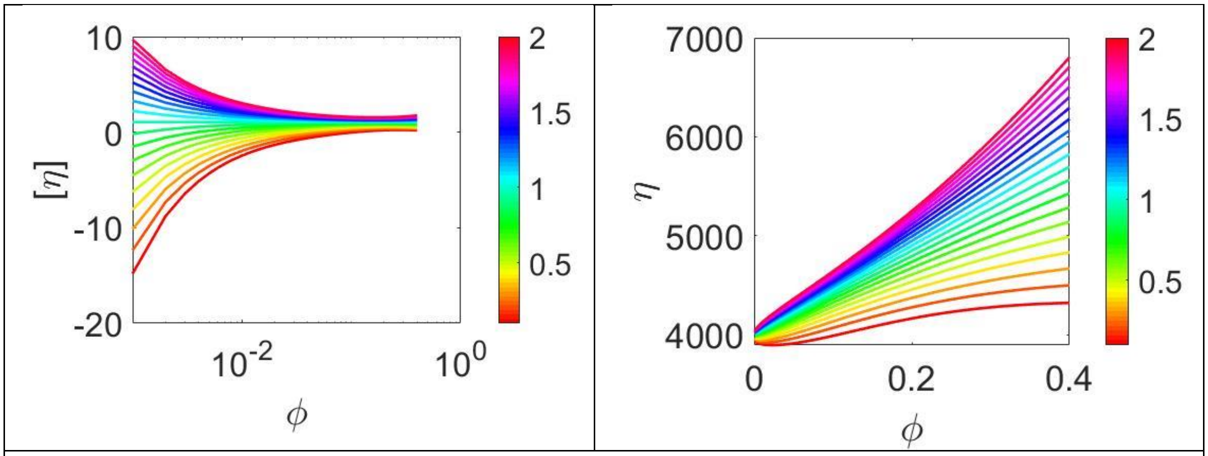

Fig. S12: (left) Intrinsic viscosity as a function of φ with varying χ. The color bar represents the values of χ. (right) Corresponding viscosity estimated using the relation 3.

Using the above equation, we have calculated the viscosity with varying χ to compare our result at different *f* values and presented in Fig. 4 of the main manuscript.

In order to compare this model with our experimental observation, we performed the calculation for a large range of χ values e.g. 0.0001 to 10 which is significantly large with respect to expected χ values for a standard polymer nanocomposite [6, 8] which is shown in Fig. S13 using pure polymer viscosity as $4*10^3$ (a.u).

The result shows distinct regimes of increase and decrease in composite viscosity obtained by changing the values of χ similar to the experimental observation of PNCs with different *f* values. However, a closer look at the data reveals that only at a very small value of χ (= 0.0001), orders of magnitude smaller than the suggested value of χ for similar composite systems in Ref. 6 and 8, the viscosity shows a drastic reduction at the high volume fractions (= 0.8). Although qualitative behavior appears similar the actual quantitative comparison with our experimental data for low f (=0.15) case is quite poor.

On the other hand, as the value of χ increases, the behavior of the composite alters and thus exhibits an enhanced viscosity which is similar to our experimental observation for high *f*. However, the extent of viscosity change at a very high value of χ (~ 10), which is significantly higher than the expected value for a similar PNC [6,8], is yet smaller than our experimental observation for PNC with *f* = 1.

Despite the fact that quantitative agreement is lacking between our experiments and the WH model in general we can observe that in this model low *f* regime in our experiments might correspond to low χ (although unreasonably low) while high *f* values might correspond to very high χ (although unreasonable).

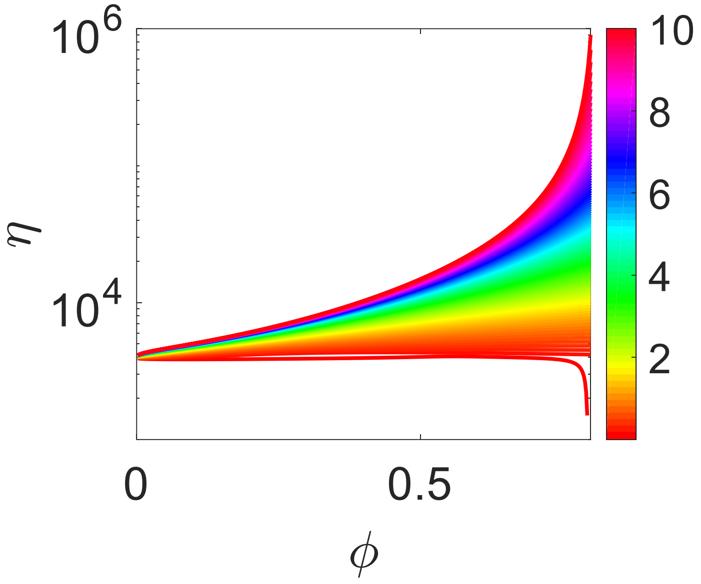

Fig. S13: Viscosity (in a.u.) of polymer nanocomposite as a function nanoparticle volume fraction for varying χ values (from 0.0001 to 10) as indicated by the color bar.

References:

1. S. Chandran, N. Begam, V. Padmanabhan, J. K. Basu, Nat. Commun. 2014, 5, 1-9.
2. M. K. Corbierre, N. S. Cameron, M. Sutton, K. Laaziri, R.B. Lennox, Langmuir, 2005, 21, 6063–6072.
3. H.W. Fox, P.W. Taylor, and W.A. Zisman, *Ind. Eng. Chem.* 1947, **39**, 1401.
4. X. Ye, D. Cai, X. Ruan, A. Cai, *AIP Advances* 2018, **8**, 095004.
5. M. Wang, R. J. Hill, Soft Matter 2009, 5, 3940–3953.
6. S. Cai and B. Bhushan, Nanotechnology, 2017, 18, 465704 (14pp).
7. H. Kim, A. Rühm, L.B. Lurio, J. K. Basu, J. Lal, D. Lumma, S. G. J. Mochrie, S. K. Sinha, Phys. Rev. Lett. 2003, 90, 068302.
8. A. Tuteja, M. E. Mackay, C. J. Hawker and B. Van Horn, *Macromolecules*, 2005, **38**, 8000–8011.